Chemical Research in Toxicology

ARTICLE

pubs.acs.org/crt

Toxicity of Multiwalled Carbon Nanotubes with End Defects Critically Depends on Their Functionalization Density

Sanyog Jain,*[,†] Vivek S. Thakare,[†] Manasmita Das,[†] Chandraiah Godugu,[†] Amit K. Jain,[†] Rashi Mathur,[‡] Krishna Chuttani,[‡] and Anil K. Mishra[‡]

[†]Centre for Pharmaceutical Nanotechnology, Department of Pharmaceutics, National Institute of Pharmaceutical Education and Research (NIPER), Sector 67, SAS Nagar (Mohali), Punjab, India 160062

[‡]Division of Cyclotron and Radiopharmaceutical Sciences, Institute of Nuclear Medicine and Allied Sciences, Brig. S.K. Mazumdar Road, Timarpur, Delhi, India 110054

Supporting Information

ABSTRACT: Carboxylated carbon nanotubes stand as the most promising nanovectors for biomedical and pharmaceutical applications due to their ease of covalent conjugation with eclectic functional molecules including therapeutic drugs, proteins, and oligonucleotides. In the present study, we attempt to investigate how the toxicity of acid-oxidized multiwalled carbon nanotubes (MWCNTs) can be tweaked by altering their degree of functionalization and correlate the toxicity trend with their biodistribution profile. In line with that rationale, mice were exposed to 10 mg/kg of pristine (p) and acid-oxidized (f) MWCNTs with varying degrees of carboxylation through a single dose of intravenous injection. Thereafter, extensive toxicity studies were carried out to comprehend the short-term (7 day) and long-term (28 day) impact of p- and various f-MWCNT preparations on the physiology of healthy mice. Pristine MWCNTs with a high aspect ratio, surface hydrophobicity, and metallic impurities were found to induce significant hepatotoxicity and oxidative damage in mice, albeit the damage was recovered after 28 days of treatment. Conversely, acid-oxidized carboxylated CNTs with shorter lengths, hydrophilic surfaces, and high aqueous dispersibility proved to be less toxic and more biocompatible than their pristine counterparts. A thorough scrutiny of various biochemical parameters, inflammation indexes, and histopathological examination of liver indicated that toxicity of MWCNTs systematically decreased with the increased functionalization density. The degree of shortening and functionalization achieved by refluxing p-MWCNTs with strong mineral acids for 4 h were sufficient to render the CNTs completely hydrophilic and biocompatible, while inducing minimal hepatic accumulation and inflammation. Quantitative biodistribution studies in mice, intravenously injected with Tc-99m labeled MWCNTs, clearly designated that clearance of CNTs from reticuloendothelial system (RES) organs such as liver, spleen, and lungs was critically functionalization density dependent. Well-individualized MWCNTs with shorter lengths (<500 nm) and higher degrees of oxidation (surface carboxyl density >3 μmol/mg) were not retained in any of the RES organs and rapidly cleared out from the systematic circulation through renal excretion route without inducing any obvious nephrotoxicity. As both p- and f-MWCNT-treated groups were devoid of any obvious nephrotoxicity, CNTs with larger dimensions and lower degrees of functionalization, which fail to clear out from the body via renal excretion route, were thought to be excreted via biliary pathway in faeces.

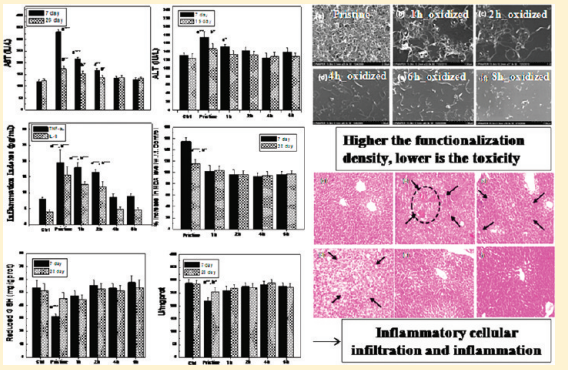

1. INTRODUCTION

Carbon nanotubes (CNTs) represent a novel class of nanomaterials that stepped into the nanomedicine arena not more than a decade back. Nevertheless, their unique properties such as a high aspect ratio, ultralight weight, ease of drug loading via $\pi-\pi$ stacking interactions, and photoacoustic effects have made them potential candidates for targeted drug delivery and diagnostic imaging.[1,2] Although CNTs have shown considerable promise in the biomedical field, their application in vivo is often fraught with certain toxicological concerns, closely associated with their high aspect ratio as well as hydrophobicity of the graphene side walls. These two factors, coupled with strong $\pi-\pi$ interactions between the individual tubes, cause pristine CNTs to assemble as bundles, rendering them water-insoluble and subsequently toxic. One of the most promising approaches for enhancing the dispersibility of CNTs in a wide variety of solvents is to covalently functionalize their side walls and tips. This can be implemented in a number of ways including acid-induced oxidation, 1,3-dipolar cycloaddition with azomethine ylides, diazonium salt addition, and reductive alkylation using lithium and alkyl halide.[3−5] Despite the availability of a wide range of

Received: August 29, 2011
Published: October 06, 2011

functionalization methods, oxidation of CNTs using strong mineral acids is the most common and facile approach for concomitant removal of metal contaminants from CNTs and their subsequent enrichment with carboxyl groups. By far, carboxylated CNTs stand as the most convenient bioconjugating precursor for covalent linking with therapeutic drugs, proteins, and oligonucleotides. The interest in carboxylated CNTs is largely indebted to their ease of preparation and ready interchangeability with other functional groups. Furthermore, depending on the applications and the number of bioactives to be attached with CNTs, the surface carboxyl density can be easily modulated by simple manipulation of reaction and process variables. Despite the popularity of carboxylated CNTs as a promising nanovector for biomedical and pharmaceutical applications, available reports on their toxicity are highly inconsistent and disputed, too. For example, Bottini et al. have compared the toxicity of pristine and oxidized CNTs on T lymphocytes and found that the latter were more toxic and induced a massive loss of cell viability through programmed cell death at a dose of 400 μg/mL.[6] Similarly, Patlolla et al. have shown that more hydrophobic nonfunctionalized/pristine CNTs are less toxic than their functionalized/oxidized counterparts in inducing genotoxic/clastogenic effects in bone marrow cells.[7] Conversely, there are examples in the literature in which functionalized CNTs have been reported to be more biocompatible and less toxic than their pristine counterparts.[8] These conflicting data highlight the need to revisit the toxicity of pristine and carboxylated CNTs and ensure the safety of the latter with context to in vivo applications. Furthermore, in a recent report, Yang et al. have demonstrated that covalently PEGylated SWCNTs could be slowly defunctionalized in liver via enzymatic hydrolysis or radical attack and return to oxidized CNTs.[9] Therefore, it is quite feasible that the in vivo toxicity of any covalently functionalized CNTs with defects, in the long term, may arise from the oxidized CNTs. Unfortunately, biodistribution and toxicity of carboxylated CNTs in vivo have been seldom investigated. For example, Liu et al. have demonstrated that carboxyl functionalization reduces the hepatotoxicity of MWCNTs in mice. However, they have not set any lower limit for the degree of functionalization that is ideally required to ensure safe administration of CNTs into the body, while inducing minimal tissue accumulation and inflammation.[10] This is particularly important because cell responses to CNTs critically depend on the degree of functionalization. In fact, there are reports according to which an increase in the surface density of acidic functional groups ($-SO_3H/-CO_2H$) can increase the cytotoxic response of CNTs in vitro.[11] The present study stemmed from the need to fully address the toxicology of acid-oxidized, carboxylated CNTs, particularly in comparison with the pristine ones, and concomitantly investigate whether and how this toxicity profile can be tweaked by altering the density of surface functional groups. Because acid oxidation is the most commonly employed technique for introducing carboxyl functions on CNTs, we sought to understand how the oxidation time influenced the length, hydrophilicity, surface potential, and carboxyl densities associated with the nanotubes and tried to correlate the particle characteristics of CNTs with their toxicities and biodistribution profiles. In line with that objective, mice were intravenously injected with pristine (p) and acid-oxidized (f) MWCNTs with varying degrees of carboxylation. Thereafter, functionalization density dependence of oxidized MWCNTs on various toxicological parameters was critically examined to comprehend the short-term (7 days) and long-term (28 days) impact of p- and various f-MWCNT preparations on the physiology of healthy mice. Finally, quantitative biodistribution studies were undertaken to apprehend how the degree of functionalization of MWCNTs influences their biodistribution and clearance from major organs of the body and, in turn, their toxicity profile.

2. EXPERIMENTAL PROCEDURES

2.1. Materials. Pristine multiwalled CNTs were obtained as a gift sample from Nanovatec Pvt. Ltd. (United States), while sulfuric acid and nitric acid (69−72%) were purchased from Loba Chemie Pvt. Ltd. (Mumbai, India). Diagnostic Kits (AST, ALT) were procured from Accurex Biomedical Pvt. Ltd. (Mumbai, India). All other chemicals and solvents were of analytical grade and procured from local suppliers unless otherwise mentioned.

2.2. Functionalization of Pristine CNTs. Pristine MWCNTs (50 mg) were dispersed in 20 mL of H_2SO_4:HNO_3 in a ratio of 1:3. The dispersion was sonicated for 5 min to debundle the aggregates and get a uniform dispersion. Thereafter, the dispersion was refluxed at 80 °C using hot plate stirrer at 900 rpm. Oxidation was carried out for 1−8 h to ensure different degrees of functionalization on the surface of MWCNTs. Following oxidation, dispersion in acids was diluted up to five times its volume and centrifuged to isolate the functionalized product from the mother liquor. This washing process was continued (3−4 times) until complete removal of the acid. The functionalized MWCNTs (f-CNT) obtained were dispersed in acetone, centrifuged, isolated from the centrifugate, and finally dried in a vacuum oven at 50 °C.

2.3. Characterization of Functionalized CNTs. Hydrodynamic size and ζ-potential measurements were done using the Malvern Zeta Sizer (Nano ZS, Malvern Instrument, United States). The changes in the morphology of CNTs during functionalization (oxidation) were followed up using scanning electron microscopy (SEM, model S30400). The surface chemistry of the functionalized nanotubes was studied using Fourier transform infrared (FTIR) spectroscopy and thermogravimetric analysis (TGA). FTIR spectra were recorded on Perkin-Elmer systems using KBr pellets and processed using Spectrum Software. TGA was carried out on a Perkin-Elmer System by heating 5 mg of p- and f-CNT at the rate of 10 °C/min. The contact angle was recorded by a contact angle goniometer using static sessile drop method.

2.4. In Vivo Toxicity Studies. *2.4.1. Animals and Treatment: General Experimental Design.* The toxicity study was carried out in male Swiss mice (weighing ∼25 g). The animals were divided into six groups with each group containing eight animals. Pristine MWCNTs (solubilized in 0.1% pluronic) and f-MWCNTs (suspended in saline) were administered in different groups of mice (n = 8) through a single dose of intravenous injection via the tail vein. The mice were housed in plastic cages, fed with a commercial diet, and given water ad libitum. The cages were placed in a conventional room, which was air-conditioned at 23 °C with 55−70% humidity and a 12 h light/12 h dark cycle. All animal experiments were performed in compliance with the regulations of institutional animal ethics committee of NIPER. After the mice were exposed by intravenous injection, general conditions including appetite, activity, and body weight were monitored and recorded at regular intervals. At the end of 7th and 28th days, blood was collected through cardiac puncture to analyze the various biochemical parameters and inflammation indexes. Thereafter, animals were humanely sacrificed, and the individual organs (viz. liver, spleen, kidney, and lungs) in the control as well as treated groups were excised and weighed to determine the organ indices. The organ index, which is a marker of general organ level toxicity, was measured by calculating the ratio of increase in organ weight due to inflammation and cellular infiltration to the reduction in total body weight. All results, unless otherwise stated, are expressed as means ± standard deviations (SDs).

2.4.2. Determination of Serum Biochemical Parameters and Inflammation Indexes. Aspartate transaminase (AST) and alanine transaminase (ALT) level in serum were analyzed using commercially available kits (Accurex, Biomedical Pvt. Ltd.) following manufacturer's instructions. Briefly, a working solution was prepared according to the procedure supplied along with the kits. For the assay, serum (0.1 mL) was thoroughly mixed with working solution (1 mL). Thereafter, the assay mixture was transferred to a thermostatted cuvette, and immediately, the stop watch was started. The first reading was recorded at the 60th second and subsequently three more readings with 30 s intervals at 340 nm. The activity of AST in IU/L was calculated as AST (IU/L) = ΔAbs/min × 1749.

Tumor necrosis factor-α (TNF-α) (mouse TNF-α ELISA kit, catalogue no. 88-7342-29, e-Bioscience Inc., San Diego, CA) and interleukin-6 (IL-6) (mouse IL-6 ELISA kit, catalog no. 88-7964-29, e-Bioscience Inc.) levels were measured by enzyme-linked immunoassay (ELISA) method, as per the manufacturer's instructions. Cytokine levels were expressed as pg/mL plasma.

2.4.3. Oxidative Stress Parameters. 2.4.3.1. Lipid Peroxidation in Liver: TBARS Estimation. The malondialdehyde (MDA) content, a measure of lipid peroxidation, was assayed in the form of thiobarbituric acid reacting substances (TBARS) by the method reported by Okhawa et al.[12] Briefly, 100 μL of tissue homogenate was mixed with 100 μL of SDS (8.1%), 750 μL of thiobarbituric acid (0.8%), and 750 μL of 20% glacial acetic acid (pH 3.5). Excised livers from mice were homogenized in 5 volumes of ice cold PBS (pH 7.4) using a polytron homogenizer. The total homogenate was used for the MDA estimation. The spectrophotometric method as reported in the literature was followed for MDA estimation. Briefly, 100 μL of tissue homogenate was mixed with 100 μL of SDS (8.1%), 750 μL of thiobarbituric acid (0.8%), and 750 μL of 20% glacial acetic acid (pH 3.5). The contents were mixed and boiled at 100 °C for 1 h followed by cooling to room temperature, and the contents were centrifuged at 10000*g* for 5 min to collect the supernatant. The absorbance of supernatant was measured at 532 nm. MDA standards of various concentrations were used for the standard curve. From the standard curve, MDA levels were measured and expressed as nmol (nM) MDA/mg protein.

2.4.3.2. Reduced Glutathione (GSH) Level and Superoxide Dismutase (SOD) Activity in Liver. GSH and SOD are important antioxidants in living creatures, which protect organisms by scavenging free radicals. To determine the reduced GSH level or SOD activity in liver, fresh livers excised from various treated groups were immersed in cold saline, blotted with filter paper, weighed quickly (for determination of liver indices), and then homogenized in ice-cold preparation buffer (1 mM Tris-HCl + 0.1 mM EDTA-2Na + 0.8% NaCl, pH 7.4) to yield 10% (w/v) homogenate. Homogenates were centrifuged at 2000 r min^{-1} for 8 min at 4 °C, and the supernatants were used immediately for the assays or stored at −80 °C until used for assay. The concentrations of reduced GSH in the supernatants were determined by using spectrophotometric diagnostic kits (Accurex, Biomedical Pvt. Ltd.) based on the method of Jollow et al.[13] using 5,5-dithiobis-2-nitrobenzoic acid for color development. Concentrations of reduced GSH were calculated by comparison with a standard curve of 0.5 $mmol^{-1}$ GSH solution. Total SOD levels in the supernatant were also determined by using spectrophotometric diagnostic kits (Accurex, Biomedical Pvt. Ltd.) based on the method of Beauchamp and Fridovic,[14] which were compared with a standard curve of 10 $\mu g\ mL^{-1}$ SOD solution.

2.4.4. Histopathological Examination of Liver. For histopathological examination of liver, a part of the liver tissues were fixed in 10% neutral buffered formalin, subjected to tissue processing, and subsequently embedded in paraffin and sectioned into slices with 5 μm thickness (Leica, Wetzlar, Germany) and stained with hematoxylin and eosin (H and E) for microscopic examination (Olympus, Tokyo, Japan).

2.4.5. Determination of Nephrotoxicity Parameters. Serum albumin and blood urea nitrogen (BUN) levels were analyzed using commercially available albumin and BUN kits purchased from Accurex, Biomedical Pvt. Ltd.

2.5. Quantitative Biodistribution Studies. *2.5.1. Radiolabeling of MWCNTs with ^{99m}Tc.* An aqueous suspension of pristine MWCNTs (in 1% Tween 80) and f-MWCNTs with different degrees of oxidation were radiolabeled with ^{99m}Tc by a direct labeling method using stannous chloride ($SnCl_2$) as the reducing agent.[15−18] Briefly, 0.1 mL of sodium pertechnetate ($^{99m}TcO_4^-$, approximately 2 μCi, obtained by solvent extraction method from molybdenum) was mixed with 50 mL of $SnCl_2$ solution (defined concentration to give 25−200 mg of $SnCl_2$ in 50 mL) in 10% acetic acid solution to reduce technetium. The solution pH was adjusted to 6.5−7.0 using 0.5 (M) sodium bicarbonate solution. To this mixture, 1 mL of MWCNT suspension (1 mg/mL) was added and incubated for 15 min at room temperature. This procedure could also lead to the formation of radio colloids (reduced and hydrolyzed Tc-99m, TcO_2) that were separated from the radiolabeled formulations by centrifugation and repeated washing with distilled water. The purified radiolabeled formulations, thus obtained, were stored in sterile evacuated sealed vials for subsequent studies.

2.5.2. Labeling Efficiency and in Vitro Stability. The labeling efficiency of the purified radiolabeled formulations was determined by ascending instant thin layer chromatography (ITLC) using silica gel (SG)-coated fiber sheets of approximately 10 cm in length (Gelman Science Inc., Ann Arbor, MI). The ITLC was performed using 100% acetone as the mobile phase. A tiny drop (2−3 mL) of the radiolabeled formulation was applied at a point 1 cm from one end of an ITLC-SG strip. The strip was developed in acetone, and the solvent front was allowed to reach approximately 8 cm from the origin. The strip was cut into two equal halves, and the radioactivity in each segment was determined in a well type γ-ray counter (γ-ray scintillation counter, Type CRS 23C; Electronics Corporation of India Ltd., Mumbai, India). The free $^{99m}TcO_4^-$ was eluted along with the solvent (R_f = 0.9), while the radiolabeled formulation remained at the point of application. The percentage (%) labeling efficiency was calculated using the following formulas: % labeling efficiency = B × 100/(T + B), where T and B represent the counts at the top and bottom, respectively. For the determination of in vitro stability, 100 μL of the labeled drug/formulations was mixed with 2.0 mL of PBS (pH 7.4) and incubated at room temperature, and the change in labeling efficiency was monitored over a period of 24 h by ITLC as described before.

2.5.3. Organ Distribution Studies. Biodistribution of the ^{99m}Tc-labeled MWCNTs was evaluated in male Swiss mice, weighing 25−30 g each. The protocol for biodistribution studies was duly approved by the institute animal ethical committee (IAEC) of Institute of Nuclear Medicine and Allied Science (INMAS), Delhi. The mice were divided into six groups of 12 animals each (total 72 mice, four mice each for one time interval). Each mouse received 100 μCi (100 μL) doses of the labeled formulations by separate intravenous injection through the tail vein. The mice were humanely sacrificed at 0.5, 2, and 24 h after the injection. The blood was collected by cardiac puncture. Subsequently, different organs like heart, lung, liver, kidney, spleen, bone, stomach, intestine, tumor, and muscle were dissected, washed with Ringer's solution to remove any adherent debris and dried using tissue paper. The organs were taken in preweighed tubes, which were weighed again to calculate the weight of organ/tissue, and the radioactivity corresponding to them was measured using a well type γ-scintillation counter. The results were expressed as percentage of injected dose (ID) per gram of organ.

2.6. Statistical Analysis. All data unless otherwise specified are expressed as means ± SDs. Statistical analysis was performed with Graph Pad Prism software (version 4.03, United States) using one-way ANOVA, followed by Tukey−Kramer multiple comparison test. $P < 0.05$ was considered statistically significant.

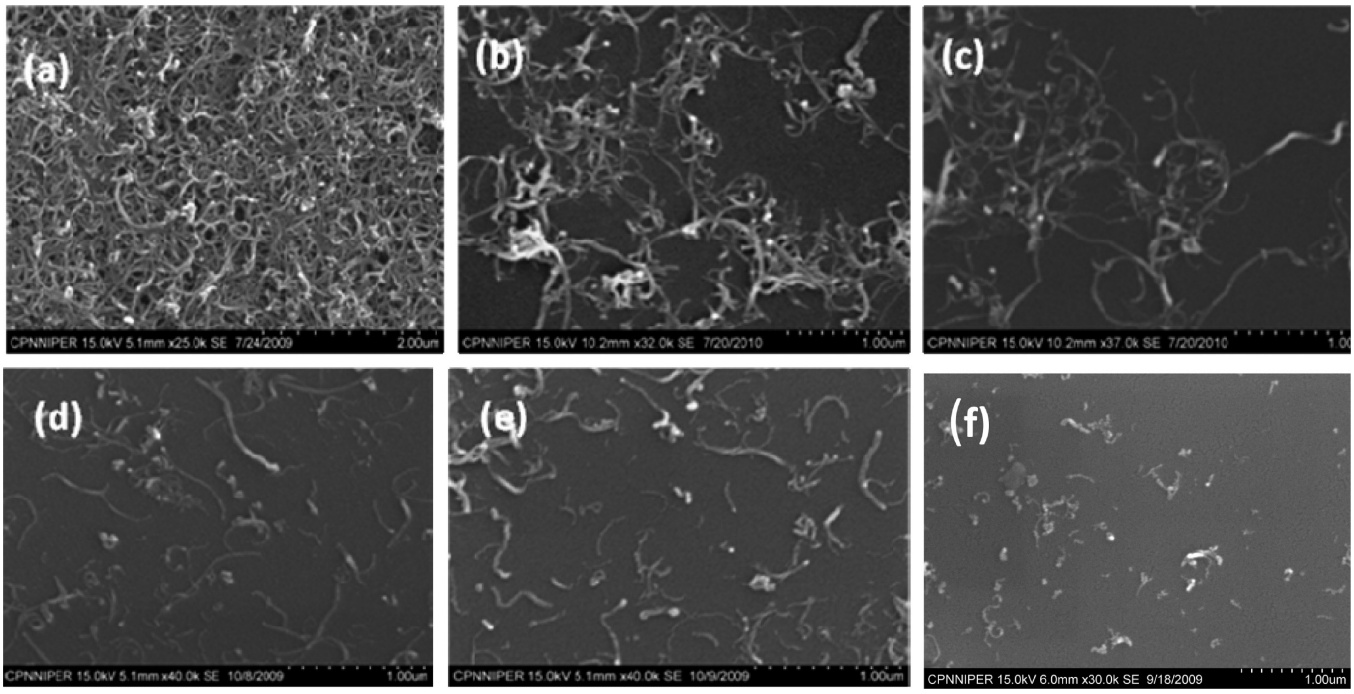

Figure 1. Scanning electron micrograph of (a) pristine MWCNTs and MWCNTs acid-oxidized for (b) 1, (c) 2, (d) 4, (e) 6, and (f) 8 h.

Table 1. Particle Characteristics of Various MWCNT Preparations

oxidation time (h)	length (μm)	structural integrity	DLS based size (nm)	−COOH density (μmol/mg)	ζ-potential (mV)	contact angle (°)
0	aggregates	unaffected	aggregates	0.00	−6.8	78.91
1	aggregates	unaffected	aggregates	2.23	−12.2	45.49
2	1−2	unaffected	516.6	2.27	−22.1	36.93
4	0.6−2.2	unaffected	423.6	3.40	−31.8	29.26
6	0.3−1	unaffected	272.4	6.00	−38.4	24.11
8	<1	affected	93.26	>6.00	−33.2	22.86

3. RESULTS AND DISCUSSION

3.1. Characterization of p-MWCNTs and f-MWCNTs. Pristine CNTs have poor solubility in most of the solvents. Functionalization through acid-induced oxidation results in the generation of surface −COOH groups with concomitant shortening of nanotubes. As shown by FTIR spectral analysis (Figure 1), pristine MWCNTs (p-MWCNTs) revealed almost flat spectra, indicative of the absence of detectable functional groups. Following oxidation, a prominent band at around 1640 cm^{-1} appeared, the intensity of which increased proportionally with the oxidation time and was easily correlable to the increase in surface carboxyl density associated with nanotubes. The physicochemical properties of p-MWCNTs and f-MWCNTs have been summarized in Table 1, which elucidates that the ζ-potential of f-MWCNTs becomes more and more negative with an increase in the oxidation time, and concomitantly, the hydrodynamic size became smaller because of shortening and debundling of CNTs. Results of SEM imaging (Figure 2) corroborated that p-MWCNTs were highly prone toward aggregation. Conversely, f-MWCNTs with a carboxyl density greater than 2.3 μmol/mg were relatively well-dispersed, and the dispersibility, as expected, was directly proportional to the degree of functionalization or, in other words, the oxidation time. As the oxidation time was increased from 0 to 6 h, the average length of CNTs gradually decreased from 10 μm to as short as 0.5 μm with no apparent change in diameter. Oxidation beyond 6 h, of course, led to further shortening of the nanotubes but was simultaneously accompanied with a loss in structural integrity. Representative transmission electron micrographs of pristine and 6 h oxidized CNTs have been presented in Figure S1 (Supporting Information). Consistent with the results of SEM analysis, TEM micrographs clearly show that acid oxidation of MWCNTs for 6 h under reflux condition is accompanied with significant shortening of length, but integrity of the side walls of nanotubes remained more or less intact.

To quantify how the degree of carboxylation increased with increase in oxidation time, TG analysis of f-CNTs was performed. Qualitatively, a TG thermogram exhibited decomposition in the range of 150−350 °C (confirmed by first order derivative), consistent with the loss of carbon dioxide resulting from decarboxylation of the surface carboxyl groups (Figure 3). This loss was directly correlated to the −COOH content of f-MWCNTs, and quantitative studies elucidated that an increase in oxidation time was accompanied with a steady increase in surface carboxyl density. This possibly led to a continuous increase in the surface hydrophilicity that was confirmed through the measurement of contact angles of the various CNT preparations (Table 1). While pristine MWCNTs exhibited a contact

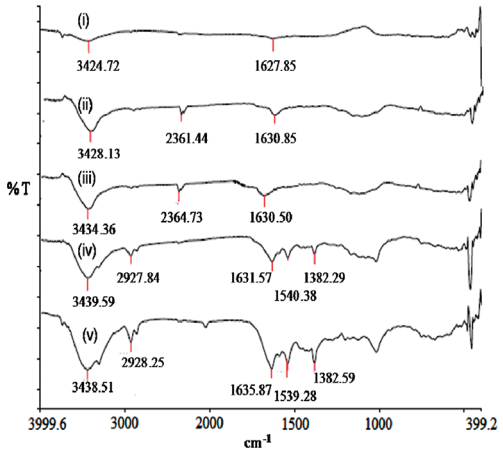

Figure 2. FTIR spectra of (i) pristine MWCNT and (ii−v) MWCNTs oxidized for 1, 2, 4, and 6 h, respectively.

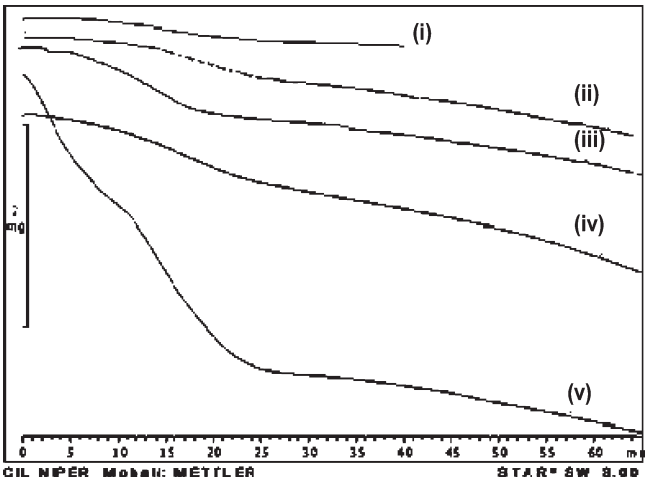

Figure 3. TG thermogram of (i) pristine MWCNT and (ii−v) MWCNTs oxidized for 1, 2, 4, and 6 h, respectively.

angle of 78.91° that represents an almost hydrophobic surface, the value dramatically reduced to 45.49° after 1 h of oxidation. After 2, 4, and 6 h of oxidation, the contact angles further decreased to 36.93, 29.26, and 24.11°, respectively, implying that carboxyl enrichment of pristine MWCNTs was accompanied with a marked increase in surface hydrophilicity. As evident from contact angle data, surface hydrohilicity continuously increased with increase in carboxyl density of MWCNTs, albeit the change was less pronounced over the course of 2−6 h of oxidation.

3.2. General Toxicity. As a preliminary step toward toxicity evaluation, we scrutinized the general health conditions of mice following 7 and 28 days of intravenous injection. Even after treatment for 28 days, mice exposed to f-MWCNTs appeared lively without any obvious alterations in vocalization, labored breathing or difficulties in movement, hunching, and interactions with cage mates. Conversely, mice treated with p-MWCNTs appeared somewhat lethargic and congregated at the corner of the cage just after day 1 of treatment. Comparison of the body weight before and after treatment with various CNT preparations revealed significant differences between the control and the p-MWCNT-exposed groups, indicating potential toxicity of p-MWCNTs, whereas differences between the control and the f-MWCNT-treated groups steadily mitigated with increased degree of functionalization (data not shown). Organ indices of p- and f-MWCNT-injected mice, 7 and 28 days post-treatment, have been presented in Figure 4. In either case, organ indices gradually decreased with increased degree of functionalization and finally approached near to that of the control group, suggesting that biocompatibility of CNTs improve with an increase in functionalization density. While p-CNTs with larger size and poor dispersibility were more prone toward agglomeration and educed cellular responses, carboxylated CNTs with better aqueous dispersibility and shorter length could easily translocate across the organs inducing minimal cellular responses or inflammation. The results are in line with a previous report by Kosteralos et al., which shows that the higher the degree of functionalization of ammonium-functionalized MWCNTs (MWNT-NH_3^+), the lower is their tissue accumulation.[19] It should, however, be noted that kidney remained unaffected in all of the groups, indicating the least or no involvement of kidneys toward the CNTs.

3.3. Biochemical Parameters and Inflammation Index in Blood. Liver is the major site of accumulation and metabolism for most of the xenobiotics including carbonaceous materials and other nanomaterials. Hence, any changes in liver enzymes are indicative of liver's physiological state. Serum AST and ALT are important biochemical enzymes reflecting hepatic injury.[20] AST is a pyridoxal phosphate (PLP)-dependent transaminase enzyme, which catalyzes the interconversion of aspartate and α-ketoglutarate to oxaloacetate and glutamate according to the following reaction: aspartate (Asp) + α-ketoglutarate $\rightleftharpoons$ oxaloacetate + glutamate (Glu). In the subsequent step, oxaloacetate reacts with NADH in the presence of MDH to form NAD^+ and L-malate: oxaloacetate + NADH+H^+ $\rightleftharpoons$ L-malate + NAD^+. The conversion of NADH to NAD^+ is proportional to the concentration of AST in serum and is measured at 340 nm as a rate of decrease in absorbance. Like AST, ALT catalyzes the transfer of an amino group from alanine to α-ketoglutarate, thereby producing pyruvate and glutamate: glutamate + pyruvate $\rightleftharpoons$ α-ketoglutarate + alanine. Any injury or damage to liver is associated with the elevation of AST and ALT levels. Figure 5 presents the AST levels in mouse blood, respectively, at 7 and 28 days postexposure. In either case, p-MWCNT caused maximum liver damage in mice because of their highest propensity toward agglomeration and hepatic accumulation. As evident from Figure 5, carboxyl enrichment of MWCNTs was associated with a significant depreciation of AST level, and the value decreased in function of surface carboxyl density, at least up to 4 h of oxidation. The changes, however, became statistically insignificant for mice exposed to CNTs oxidized beyond 4 h. The toxicity profile correlated well with the observed trend of hydrophilicity, determined from contact angle measurements. These observations cumulatively suggest that carboxyl enrichment of pristine MWCNTs not only enhances their surface hydrophilicity and dispersibility under physiological conditions but also facilitates their translocation across the hepatic milieu, which in turn attenuates their damaging potential. Figure 6 presents the ALT levels in mouse blood, injected with various MWCNT preparations following 7 and 28 days of intravenous injection. Consistent with the AST profile, the ALT levels of various MWCNT-treated groups exhibit clear functionalization density dependence. However, a careful scrutiny of the data reveals that the values of AST in mice treated with pristine or 1 h oxidized MWCNT were significantly higher than the corresponding

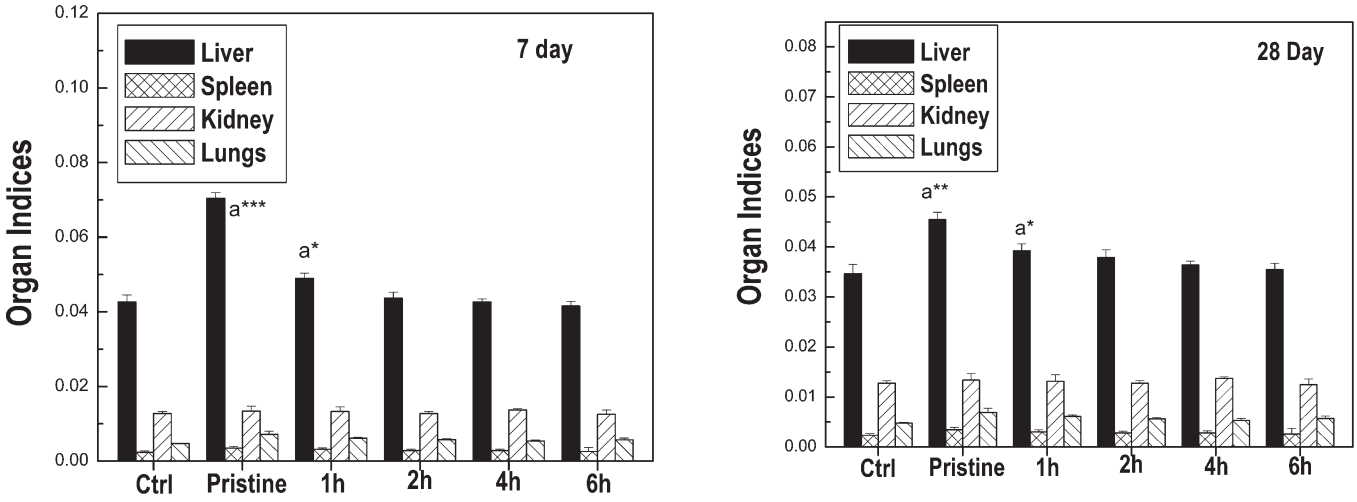

Figure 4. Organ indices of mice treated with various MWCNT preparations after 7 and 28 days. Values expressed as means ± SDs (n = 8). Values are expressed as means ± SDs (n = 8): a*, wrt control, 7 days; and b*, wrt control, 28 days (***p < 0.001, **p < 0.01, and *p < 0.05).

ALT levels. The observations can be easily justified, if we consider the basic mechanism of liver injury or metabolism dysfunction. In the hepatocyte, ALT predominantly exists in the cytosol, while AST resides in cytosol as well as mitochondria. Most of the elevated transaminases in hepatic disease reflect seepage of enzymes through damaged cell membranes, that is, the cytosol components escape leaving the mitochondria behind. Hence, the serum ALT level is likely to exceed the serum AST level. However, if the damage is severe and many hepatocytes are destroyed, then in addition to the cytosol components, the mitochondrial enzymes are released as well, giving an AST value significantly higher than the ALT value.[21] These results clearly indicate that p-MWCNTs as also f-MWCNTs with lower degree of carboxylation induce severe hepatocyte mitochondrial damage. However, the damage seemed to be partially recovered after 28 days, as AST/ALT levels of mice treated with various MWCNT preparations had only slight differences with respect to control. The results are in line with a previous report, according to which oxidative damage induced by Tween-80 dispersed MWCNTs and acid-oxidized MWCNTs at 7 days was almost completely recovered after 28 days.[10] This recovery is essentially archetypal of a single injection exposure. Initially, administration of MWCNTs is associated with marked diminution of antioxidant levels in the body, so the organisms activate their intrinsic defense pathways. By day 28 postinjection, the mice were believed to deal successfully with the administered toxins (through antioxidants, immune response cells, etc.), and the oxidative indexes gradually returned to their basal levels.

TNF-α is a multifunctional proinflammatory cytokine that belongs to the TNF superfamily. It is considered as one of the most important promoters of inflammation, necrosis, and fibrosis in liver damage.[22] Interleukin-6 (IL-6) is an interleukin that acts as both a pro-inflammatory and an anti-inflammatory cytokine. An increase in the TNF-α and IL-6 level is indicative of increased inflammation.[23] Our results showed that the TNF-α and IL-6 levels were the highest in case of p-MWCNTs, while in either case, the levels depreciated with increased degree of functionalization (Figure 7a,b), suggesting that inflammation gradually decreased as the extent of functionalization increased. Consistent with other biochemical parameters, TNF-α and IL-6 levels of mice injected with various CNT preparations depreciated after 28 days, suggesting partial recovery of CNT-induced inflammation (data not shown).

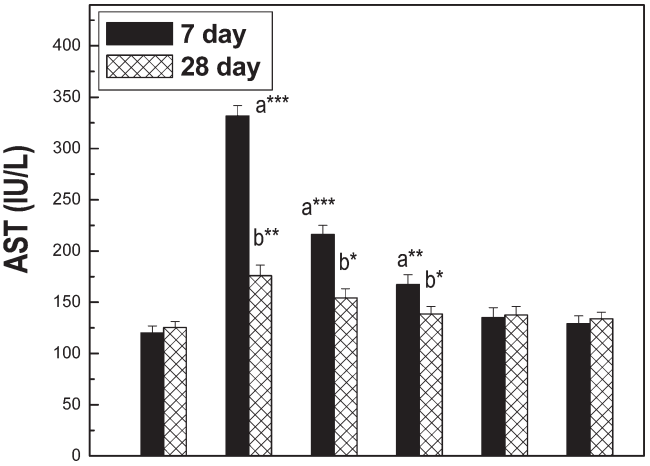

Figure 5. AST profile of mice treated with various MWCNT preparations after 7 and 28 days. Values are expressed as means ± SDs (n = 8): a*, wrt control, 7 days; and b*, wrt control, 28 days (***p < 0.001, **p < 0.01, and *p < 0.05).

3.4. Oxidative Stress Damage in Liver. Oxidative stresses arose due to the imbalance between the production of reactive oxygen species (ROS) and their degradation by antioxidants.[24] ROS interact hysterically with the cell membrane, DNA, or other cell compounds, which results in severe damage of these cell constituents. Malonaldehyde (MDA) is the lipid peroxidation product, indicative of oxidative stress, and is reactive toward thiobarbituric acid, forming a colored, spectrophotometrically determinable complex. Figure 8 presents the MDA levels in liver, following 7 and 28 days postadministration. Among all of the treatment groups, p-MWCNTs showed maximum oxidative stress, and the level of stress was quite nominal for all f-MWCNT groups. It was further interesting to note that at the end of 28 days, the MDA level of both p- and f-MWCNT-treated groups showed insignificant differences from the control, implying that oxidative stress induced by p-MWCNT after 7 days was almost recovered after 28 days.

GSH and SOD are two important antioxidants for balancing the ROS levels.[25] In healthy cells and tissue, more than 90% of

dx.doi.org/10.1021/tx2003728 |Chem. Res. Toxicol. 2011, 24, 2028–2039

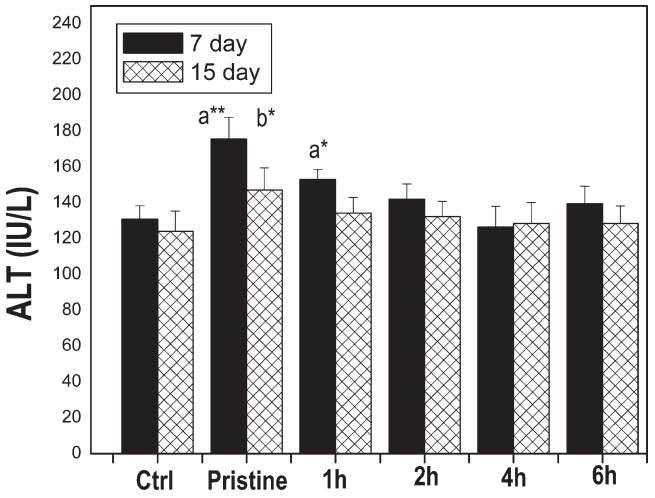

Figure 6. ALT profile of mice treated with various MWCNT preparations after 7 and 28 days. Values are expressed as means ± SDs ($n = 8$): a*, wrt control, 7 days; and b*, wrt control, 28 days (***$p < 0.001$, **$p < 0.01$, and *$p < 0.05$).

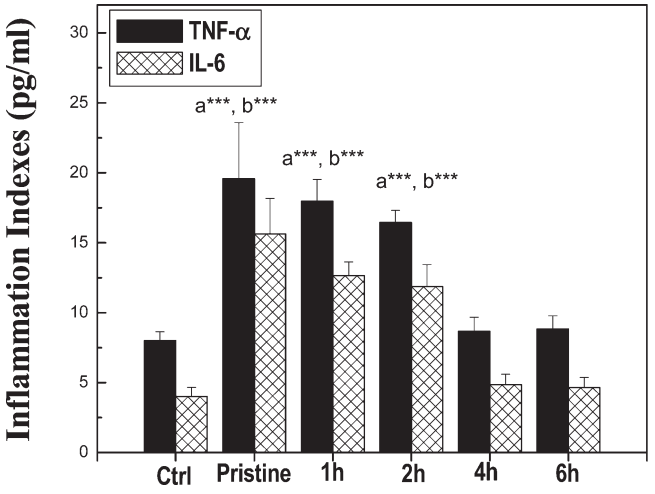

Figure 7. (a) TNF-α and (b) IL-6 of mice treated with various MWCNT preparations after 7 days. Values are expressed as means ± SDs ($n = 8$): a*, wrt control, 7 days; and b*, wrt control, 28 days (***$p < 0.001$, **$p < 0.01$, and *$p < 0.05$).

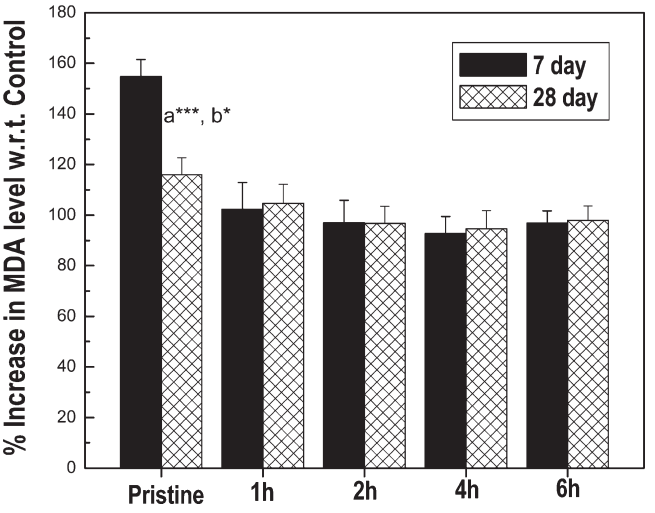

Figure 8. MDA level in the liver homogenate of mice treated with various MWCNT preparations after 7 and 28 days. Values expressed as means ± SDs ($n = 8$): a*, wrt control, 7 days; and b*, wrt control, 28 days (***$p < 0.001$, **$p < 0.01$, and *$p < 0.05$).

the total GSH pool is in the reduced form (GSH), and less than 10% exists in the disulfide form (GSSG). An increase in oxidized glutathione (GSSG), decrease in total GSH, and subsequently increase in the GSSG-to-(GSSG + GSH) ratio is considered indicative of oxidative stress. SOD represents a class of enzymes that catalyzes the dismutation of superoxide into oxygen and hydrogen peroxide. Simply stating, SOD outcompetes the deleterious reactions of superoxide, thus protecting the cells from superoxide toxicity. Figure 9a,b shows the GSH level and SOD activity in mouse liver at 7 and 28 days, respectively. As far as 7 days' data is concerned, in either case, the p-MWCNTs-treated groups exhibited significantly lower GSH level and SOD activity as compared to the control group, indicating oxidative stress. As observed in case of MDA analysis, neither GSH level nor SOD activity showed any detectable functionalization density dependence, and the stress induced by p-MWCNT after 7 days was recuperated after 28 days due to the body's natural defense mechanism. Cumulatively, MDA, GSH, and SOD profile of p- and all f-MWCNT-treated groups suggested that acid oxidation or carboxyl functionalization is crucial to alleviate the severity of oxidative stress induced by p-MWCNTs. However, in contrast to other biochemical parameters and toxicity indexes, the level of oxidative stress was independent of the degree of functionalization. To rationalize our observations, we tried to look into the oxidative stress model,[20,26] which is often proposed to predict the toxicity of engineered nanomaterials both in vitro and in vivo. Different mechanistic pathways have been proposed for CNT-induced oxidative stress. According to Sarkar et al., single-walled carbon nanotubes (SWCNTs) induced oxidative stress through the activation of a specific signaling pathway in keratinocytes.[27] However, most of the other literatures have reported that metal impurities associated with CNTs play a crucial role in the generation of ROS process.[28] In vitro studies with NR8383 and A549 cells suggested that exposure to p-MWCNTs induced cellular oxidative stress.[29] However, when the CNTs were acid-treated to remove metal contaminants, cellular ROS generation is mitigated, suggesting that metal contaminants play a crucial role in ROS generation. To verify whether p-MWCNT-induced oxidative stress in the present case was due to the presence of metallic impurities, electron dispersive X-ray (EDAX) elemental analysis of both p- and various f-MWCNT preparations was performed. While appreciable amounts of Ni (0.081 wt %), Fe (2.31 wt %), and Zn (2.29 wt %) were detected in our p-MWCNT sample, the purity of all f-in MWCNTs samples was very high. In fact, the 1 h oxidized CNTs contained only traces of Ni (0.041 wt %), Fe (0.005 wt %), and Zn (0.081 wt %), which were too low to impart any obvious toxicity. The results corroborated that metallic contaminants associated with our p-MWCNTs, particularly iron, potentiated the generation of highly reactive and toxic hydroxyl radical and induced oxidative damage. Acid oxidation for 1 h is sufficient to ensure complete removal of metallic impurities from the f-MWCNT samples. Consequently, irrespective of the density of surface functional groups, no oxidative stress was induced by the f-MWCNT batches revalidating that high purity CNTs do not incite oxidative stress. These data cumulatively suggest that intensive purification

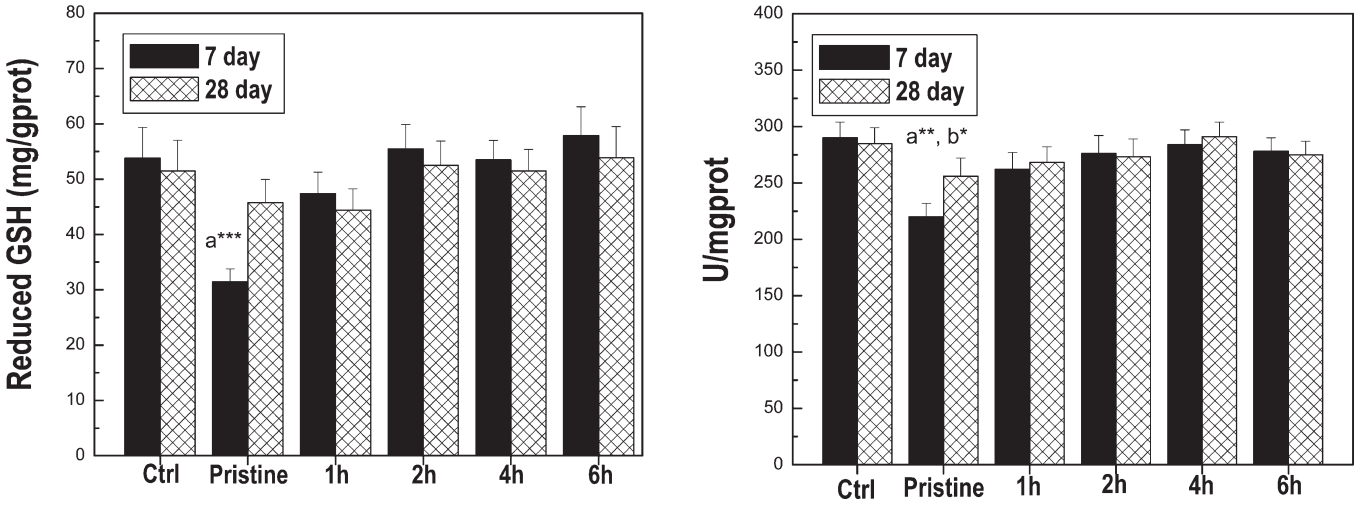

Figure 9. (a) GSH level and (b) SOD activity in liver homogenate of mice treated with various MWCNT preparations after 7 and 28 days. Values expressed as means ± SDs (n = 8): a*, wrt control, 7 days; and b*, wrt control, 28 days (***p < 0.001, **p < 0.01, and *p < 0.05).

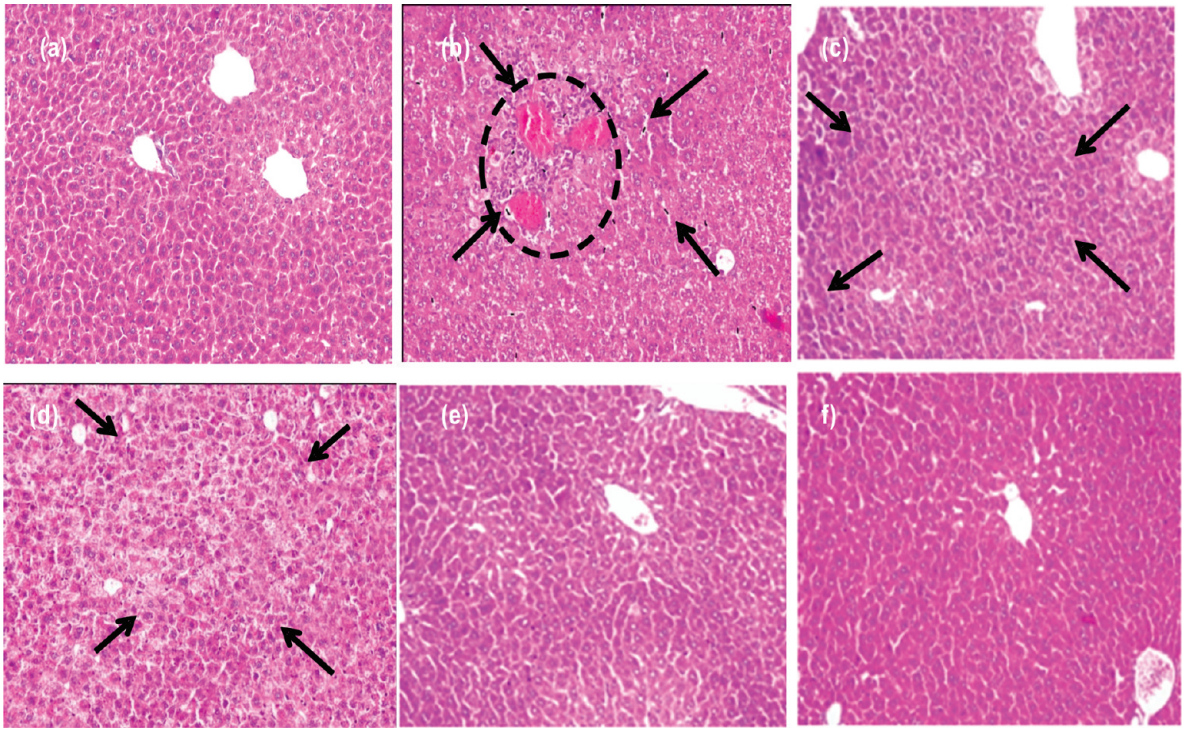

Figure 10. Histopathological images of liver sections of mice treated with (a) PBS and (b) pristine MWCNTs and MWCNTs oxidized for (c) 1, (d) 2, (e) 4, and (f) 6 h. The black arrows show inflammatory infiltrate, while the dotted circle shows inflamed regions. The extent of accumulation and inflammation decreases with increasing density of surface functional groups.

and functionalization process augments the biocompatibility of CNTs in biological system.

3.5. Histopathological Toxicity of Liver Sections. Histopathological examination of liver sections harvested after 7 and 28 days of postadministration indicated that organ accumulation critically depended on the degree of carboxyl functionalization at MWCNTs surface. As evident from the histopathological data (Figure 10a–f), carbon-based particles could be seen in the liver section of animals treated with p-MWCNTs, while the extent of accumulation gradually depreciated with increased degree of functionalization. Regarding histological toxicity, liver sections of p-MWCNT-treated groups showed severe inflammatory cell infiltration in the portal region, cellular necrosis, and focal necrosis at 7 days. On the contrary, only slight or no inflammations were envisaged in case of various f-MWCNT-treated groups; the higher the degree of functionalization, the lower was the extent of accumulation or inflammation. In line with the results of other toxicity tests, inflammation induced by p-MWCNTs was almost recovered at the end of 28 days, and no obvious damage was perceived in the liver section of various f-MWCNT-treated groups after 28 days of treatment (data not shown). The results unambiguously corroborated that p-MWCNTs

dx.doi.org/10.1021/tx2003728 |*Chem. Res. Toxicol.* 2011, 24, 2028–2039

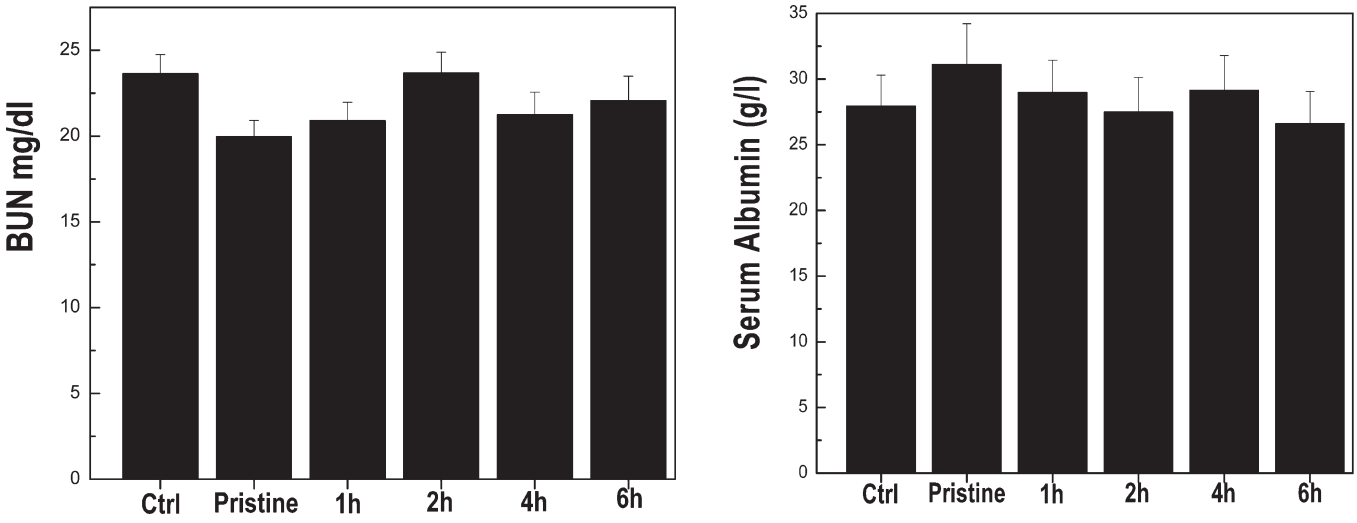

Figure 11. (a) BUN and (b) serum albumin profile of mice treated with pristine MWCNTs and MWCNTs oxidized for (c) 1, (d) 2, (e) 4, and (f) 6 h following 7 days of treatment.

were more toxic than their functionalized counterparts. An increase in surface hydrophilicity and subsequently aqueous dispersibility is believed to facilitate the translocation of MWCNTs across the membrane of hepatic cells (viz. hepatocytes and Kupffer cells) while lowering their biopersistance and interaction with lipids.

3.6. Nephrotoxicity: Serum Albumin and BUN Level. The serum albumin and BUN levels of p- and f-MWCNT treated groups after 7 days postinjection have been presented in Figure 11a,b. Interestingly, blood serum and BUN levels of both p- and f-MWCNT-treated groups were more or less similar to that of the control group, implying that MWCNTs, irrespective of their nature of surface functionality or functionalization density, did not induce any renal toxicity in mice.

3.7. Functionalization Density-Dependent Biodistribution and Clearance. Having confirmed that the toxicity of MWCNTs with end defects critically depends on their degree of functionalization, we sought to examine how the degree of functionalization influences the tissue distribution and clearance of CNTs from the major organs of the body and, in turn, their toxicity profile. In line with that idea, pristine as well as 1−6 h oxidized CNTs were labeled with Technitium-99m by direct labeling method using stannous chloride ($SnCl_2$) as the reducing agent.[15,17,18] All MWCNT preparations were labeled with more than 98% labeling efficiency and remained approximately 92−94% labeled in vitro, even after 24 h of iv injection. Figure 12 presents the comparative tissue distribution profile of pristine and f-MWCNTs with different degree of acid oxidation over time (0.5−24 h) after intravenous administration. After 0.5 h of iv injection, all MWCNT preparations, irrespective of their surface characteristics (hydrophilicity, hydrophobicity, surface charge, etc.) and carboxyl density presented an initial high accumulation (∼15−20% ID/g) in the RES organs, viz. liver, spleen, and lungs, of Qu et al.[30] according to which both agglomerated and well suspended MWCNTs are taken up by MPS organs. However, MWCNTs with a higher degree of agglomeration are predominantly retained in lungs and later in the liver for months, while the well-dispersed ones forming fewer aggregates are easily eliminated from the body via excretion. In the present case, pristine as well as 1 and 2 h oxidized CNTs presented very high activity (% ID/g) in liver, spleen, and lungs, even after 24 h of injection. On the contrary, 4−6 h oxidized CNTs with high surface-carboxyl density, were slowly cleared out from lungs, liver, and spleen over 2−24 h after iv administration, revalidating our toxicity results that well functionalized MWCNTs density exhibit the least propensity to accumulate in the liver and, therefore, are devoid of any obvious hepatotoxicity. f-MWCNTs with a higher degree of oxidation (4−6 h) also exhibited prominent % ID/g (4−5%) in the kidney over 0.5−2 h; the % ID/g abruptly declined to less than 0.5% after 24 h of treatment, indicating that well individualized CNTs may be excreted via the renal pathway. According to a recent report by Lacerda et al.,[31] in vivo transport and translocation profile of MWCNTs critically depend on their shape and degree of individualization. In the course of extensive TEM and SPECT investigations,[31,32] the same group of authors have shown that SWCNTs/MWCNTs (with diameter ∼30−38 nm) that are well individualized and soluble in biological milieu can easily translocate via their transverse dimension directly into the Bowman capsule and be excreted in urine. In our study, the length and diameter of carboxylated MWCNTs, prepared via 4−6 h of oxidation, were comparable to those reported by Lacerda and co-workers. Considering their high aqueous dispersibility, well-individualized structures, systematic clearance from the MPS organs over time, and prominent accumulation in the kidney over 0.5−2 h after iv injection, it may be assumed that these nanotubes effectively pass through the leaky tissue or fenestrations of the glomerular capillary bed (average diameter ∼70−90 nm) and excrete through the urine, without inducing any hepatic or renal toxicity. However, pristine MWCNTs, being highly hydrophobic, exhibit high propensity toward agglomeration and subsequent accumulation in the mononuclear phagocytic system (MPS) organs viz. liver, spleen, or lungs. As pristine MWCNTs and f-MWCNTs with lower degrees of oxidation showed very high accumulation (% ID/g) in the liver after 24 h of iv administration and nominal accumulation in the kidney over 0.5−4 h of treatment, it may be assumed that a very small portion of these nanotubes manage to eliminate from the body via urinary excretion and subsequently show minimal involvement with the kidney. This might be one of the plausible reasons why pristine CNTs as well as their lower oxidized counterparts did not impart any renal toxicity. As demonstrated by

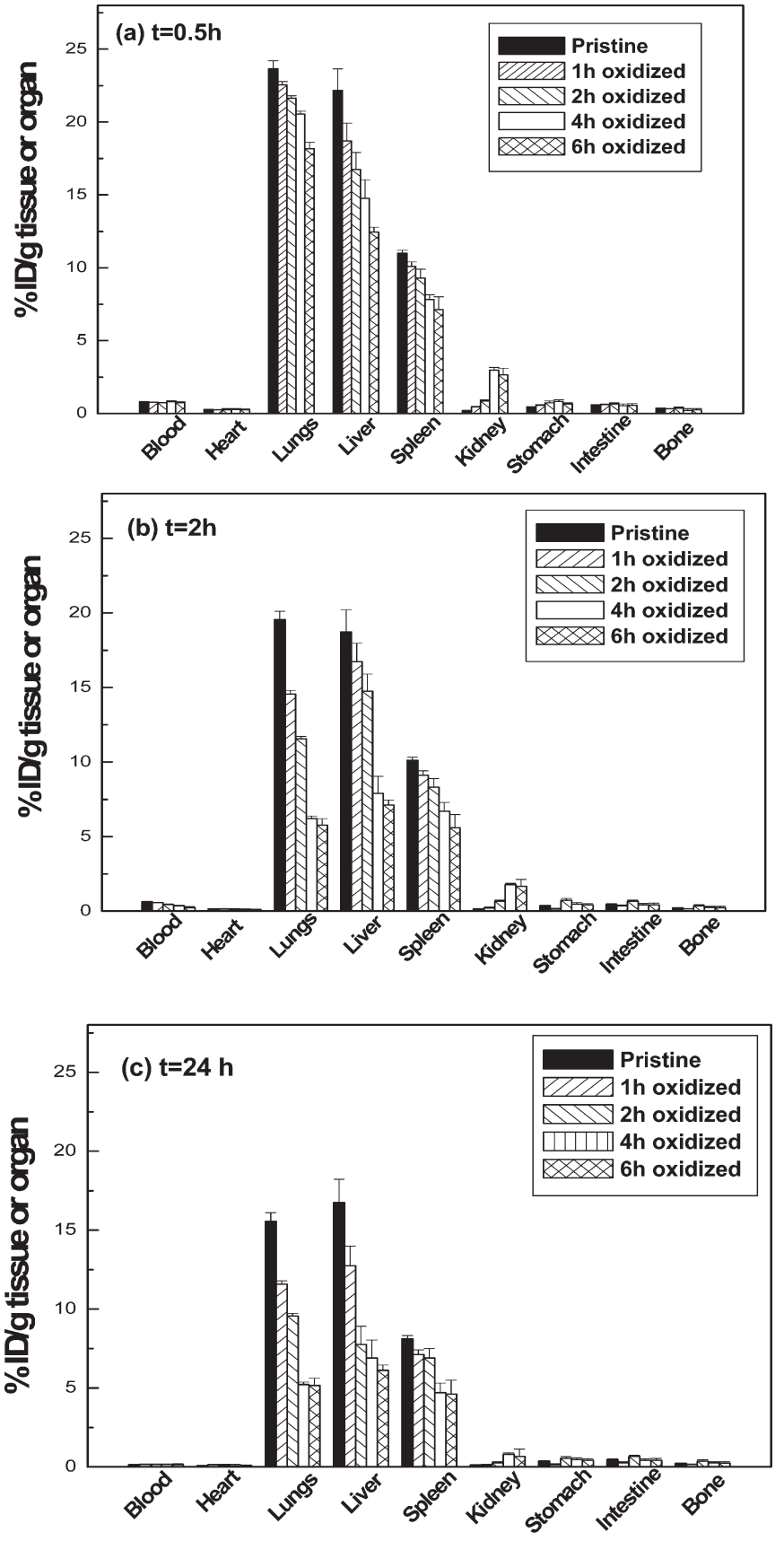

Figure 12. Functionalization density-dependent biodistribution of MWCNTs in mice after (a) 0.5, (b) 2, and (c) 24 h of intravenous injection.

dx.doi.org/10.1021/tx2003728 |*Chem. Res. Toxicol.* 2011, 24, 2028–2039

some earlier reports,[33] it is most likely that agglomerated MWCNTs of larger dimension and lower degree of individualization are possibly eliminated from the liver via the biliary pathway in the feces. Although further spectrochemical analysis of urine and faeces are required to confirm and establish the ultimate in vivo fate of the various CNT preparations, biodistribution and toxicity studies cumulatively corroborate that well-individualized CNTs with high density of surface carboxyl groups exhibit the least propensity toward biopersistence and, therefore, eliminate from the body via renal or biliary excretion. Herein, the organ distribution studies were performed over 0.5−24 h time course while short-term and long-term toxicities were evaluated after 7 and 28 days of iv administration, respectively. As both pristine and 1−2 h oxidized CNTs exhibit very high accumulation in the MPS organs, even after 24 h of injection, it may be assumed that the major portion of these CNTs are retained in the liver only, when their short-term toxicity was evaluated, that is, after 7 days of iv dosing. Conversely, considering the systematic clearance of 4−6 h oxidized CNTs from liver over 2−24 h of injection, it may be assumed that the amount of f-MWCNTs retained in the liver after 7 days of dosing will be too nominal and that also will be in a highly dispersed state to induce any major hepatic damage. However, as for long-term toxicity is concerned, the major portion of the accumulated CNTs is possibly cleared out from the liver via biliary pathways, and concomitantly, the inflammation/damage induced by pristine or 1−2 h oxidized CNTs are mostly recovered by the body's intrinsic defense mechanisms. Hence, the tissue distribution trends are in nice agreement with the observed functionalization density-dependent toxicity of MWCNTs with end defects.

4. CONCLUSIONS

Summarily, we have intensively investigated and compared the in vivo toxicity of pristine and acid-oxidized MWCNTs with varying degrees of functionalization throughout a period of 4 weeks. Pristine MWCNTs with a high aspect ratio, surface hydrophobicity, and metallic impurities were found to induce significant hepatotoxicity in mice. Conversely, acid-oxidized, carboxylated CNTs with shorter lengths, hydrophilic surfaces, and high aqueous dispersibility are less toxic and more biocompatible than their pristine counterparts. A thorough analysis of various toxicological parameters suggested that toxicity of MWCNTs critically depends on their functionalization density; the higher the density of surface carboxyl groups is, lower was the toxicity. However, the degree of shortening and functionalization achieved by refluxing p-MWCNTs with strong mineral acids for 4 h were sufficient to render the CNTs completely hydrophilic and biocompatible while evoking minimal tissue accumulation and inflammation. We observed that mice treated with 4 h oxidized CNTs (surface carboxyl density ∼3.4 μmol/mg) showed least toxicity among all of the treatment groups. No significant improvement in biocompatibility or reduction in toxicity level was perceived on further increasing the oxidation time, revalidating that extent of functionalization achieved in 4 h is enough to alleviate the toxic effects of pristine CNTs. Interestingly, CNT-induced oxidative damage was independent of functionalization density, suggesting that metal contaminants associated with pristine CNTs were responsible for the p-MWCNT evoked oxidative stress. Comparative biodistribution studies in mice, intravenously administered with Tc-99m-labeled MWCNTs, clearly indicated that tissue distribution and clearance of CNTs from the RES organs such as liver, spleen, and lungs were critically functionalization density dependent. Well-individualized MWCNTs with shorter length (<500 nm) and higher degree of oxidation (surface carboxyl density >3 μmol/mg) were not retained in any of the RES organs and rapidly cleared out from the systematic circulation through renal excretion route without inducing any obvious nephrotoxicity, while CNTs of larger dimension were predominantly excreted via the biliary pathway in feces with minimal involvement of the kidney. Overall, these findings provide some fundamental importance on the effect of oxidation and degree of surface carboxyl groups on the biodistribution, toxicity, and biocompatibility of acid-oxidized CNTs, which might be beneficial for their future biomedical applications.

■ ASSOCIATED CONTENT

Supporting Information. TEM micrograph of pristine MWCNTs and MWCNTs oxidized for 6 h. This material is available free of charge via the Internet at http://pubs.acs.org.

■ AUTHOR INFORMATION

Corresponding Author

*Tel: +91172-2292053. Fax: +91172-2214692. E-mail: sanyogjain@niper.ac.in or sanyogjain@rediffmail.com.

Funding Sources

We are thankful to the Indian Council of Medical Research (ICMR) and Department of Science & Technology (DST), Government of India, New Delhi, for financial support.

■ ACKNOWLEDGMENT

Director NIPER and Director INMAS are duly acknowledged for providing the necessary infrastructure and facilities. The technical assistance of Dinesh Singh Chauhan and Rahul Mahajan is also acknowledged.

■ REFERENCES

(1) Thakare, V. S., Das, M., Jain, A. K., Patil, S., and Jain, S. (2010) Carbon nanotubes in cancer theragnosis. *Nanomedicine 5*, 1277–1301.

(2) Pantarotto, D., Singh, R., McCarthy, D., Erhardt, M., Briand, J. P., Prato, M., Kostarelos, K., and Bianco, A. (2004) Functionalized carbon nanotubes for plasmid DNA gene delivery. *Angew. Chem. 116*, 5354–5358.

(3) Bianco, A., Kostarelos, K., and Prato, M. (2005) Applications of carbon nanotubes in drug delivery. *Curr. Opin. Chem. Biol. 9*, 674–679.

(4) Holzinger, M., Vostrowsky, O., Hirsch, A., Hennrich, F., Kappes, M., Weiss, R., and Jellen, F. (2001) Sidewall functionalization of carbon nanotubes. *Angew. Chem., Int. Ed. 40*, 4002–4005.

(5) Georgakilas, V., Kordatos, K., Prato, M., Guldi, D. M., Holzinger, M., and Hirsch, A. (2002) Organic functionalization of carbon nanotubes. *J. Am. Chem. Soc. 124*, 760–761.

(6) Bottini, M., Bruckner, S., Nika, K., Bottini, N., Bellucci, S., Magrini, A., Bergamaschi, A., and Mustelin, T. (2006) Multi-walled carbon nanotubes induce T lymphocyte apoptosis. *Toxicol. Lett. 160*, 121–126.

(7) Patlolla, A. K., Hussain, S. M., Schlager, J. J., Patlolla, S., and Tchounwou, P. B. (2010) Comparative study of the clastogenicity of functionalized and nonfunctionalized multiwalled carbon nanotubes in bone marrow cells of Swiss Webster mice. *Environ. Toxicol. 25*, 608–621.

(8) Liu, Z., Tabakman, S., Welsher, K., and Dai, H. (2009) Carbon nanotubes in biology and medicine: in vitro and in vivo detection, imaging and drug delivery. *Nano Res. 2*, 85–120.

(9) Yang, S. T., Wang, H., Meziani, M. J., Liu, Y., Wang, X., and Sun, Y. P. (2009) Biodefunctionalization of Functionalized Single-Walled Carbon Nanotubes in Mice. *Biomacromolecules 10*, 2009–2012.

(10) Ji, Z., Zhang, D., Li, L., Shen, X., Deng, X., Dong, L., Wu, M., and Liu, Y. (2009) The hepatotoxicity of multi-walled carbon nanotubes in mice. *Nanotechnology 20*, 445101.

(11) Sayes, C. M., Liang, F., Hudson, J. L., Mendez, J., Guo, W., Beach, J. M., Moore, V. C., Doyle, C. D., West, J. L., and Billups, W. E. (2006) Functionalization density dependence of single-walled carbon nanotubes cytotoxicity in vitro. *Toxicol. Lett. 161*, 135–142.

(12) Ohkawa, H., Ohishi, N., and Yagi, K. (1979) Assay for lipid peroxides in animal tissues by thiobarbituric acid reaction. *Anal. Biochem. 95*, 351–358.

(13) Jollow, D. J., Mitchell, J. R., Zampaglione, N., and Gillette, J. R. (1974) Bromobenzene-induced liver necrosis. Protective role of glutathione and evidence for 3, 4-bromobenzene oxide as the hepatotoxic metabolite. *Pharmacology 11*, 151–169.

(14) Beauchamp, C., and Fridovich, I. (1971) Superoxide dismutase: Improved assays and an assay applicable to acrylamide gels* 1. *Anal. Biochem. 44*, 276–287.

(15) Pathak, A., Kumar, P., Chuttani, K., Jain, S., Mishra, A. K., Vyas, S. P., and Gupta, K. C. (2009) Gene Expression, Biodistribution, and Pharmacoscintigraphic Evaluation of Chondroitin Sulfate- PEI Nanoconstructs Mediated Tumor Gene Therapy. *ACS Nano 3*, 1493–1505.

(16) Yadav, A. K., Agarwal, A., Jain, S., Mishra, A. K., Bid, H., Rai, G., Agrawal, H., and Agrawal, G. P. (2010) Chondroitin Sulphate Decorated Nanoparticulate Carriers of 5-Fluorouracil: Development and In Vitro Characterization. *J. Biomed. Nanotechnol. 6*, 340–350.

(17) Yadav, A. K., Mishra, P., Mishra, A. K., Jain, S., and Agrawal, G. P. (2007) Development and characterization of hyaluronic acid-anchored PLGA nanoparticulate carriers of doxorubicin. *Nanomed.: Nanotechnol., Biol. Med. 3*, 246–257.

(18) Jain, S., Mathur, R., Das, M., Swarnakar, N. K., and K., M. A. (2011) Synthesis, pharmacoscintigraphic evaluation and antitumor efficacy of methotrexate loaded, folate conjugated, stealth albumin nanoparticles. *Nanomedicine*.

(19) Lacerda, L., Ali-Boucetta, H., Herrero, M. A., Pastorin, G., Bianco, A., Prato, M., and Kostarelos, K. (2008) Tissue histology and physiology following intravenous administration of different types of functionalized multiwalled carbon nanotubes. *Nanomedicine 3*, 149–161.

(20) Murakami, S., Okubo, K., Tsuji, Y., Sakata, H., Takahashi, T., Kikuchi, M., and Hirayama, R. (2004) Changes in liver enzymes after surgery in anti-hepatitis C virus-positive patients. *World J. Surg. 28*, 671–674.

(21) Koay, E. S. C., and Walmsley, N. (1996) *A Primer of Chemical Pathology*, World Scientific Pub. Co. Inc: Singapore.

(22) Locksley, R. M., Killeen, N., and Lenardo, M. J. (2001) The TNF and TNF receptor superfamilies: Integrating mammalian biology. *Cell 104*, 487.

(23) Di Giuseppe, M., Gambelli, F., Hoyle, G. W., Lungarella, G., Studer, S. M., Richards, T., Yousem, S., McCurry, K., Dauber, J., and Kaminski, N. (2009) Systemic Inhibition of NF- B Activation Protects from Silicosis. *PloS One 4*, e5689.

(24) Nel, A., Xia, T., Mädler, L., and Li, N. (2006) Toxic potential of materials at the nanolevel. *Science 311*, 622.

(25) Lentsch, A. B., Kato, A., Yoshidome, H., McMasters, K. M., and Edwards, M. J. (2000) Inflammatory mechanisms and therapeutic strategies for warm hepatic ischemia/reperfusion injury. *Hepatology 32*, 169–173.

(26) Deng, X., Jia, G., Wang, H., Sun, H., Wang, X., Yang, S., Wang, T., and Liu, Y. (2007) Translocation and fate of multi-walled carbon nanotubes in vivo. *Carbon 45*, 1419–1424.

(27) Sarkar, S., Sharma, C., Yog, R., Periakaruppan, A., Jejelowo, O., Thomas, R., Barrera, E. V., Rice-Ficht, A. C., Wilson, B. L., and Ramesh, G. T. (2007) Analysis of stress responsive genes induced by single-walled carbon nanotubes in BJ Foreskin cells. *J. Nanosci. Nanotechnol. 7*, 584.

(28) Shvedova, A. A., Kisin, E. R., Porter, D., Schulte, P., Kagan, V. E., Fadeel, B., and Castranova, V. (2009) Mechanisms of pulmonary toxicity and medical applications of carbon nanotubes: Two faces of Janus?. *Pharmacol. Ther. 121*, 192–204.

(29) Pulskamp, K., Diabaté, S., and Krug, H. F. (2007) Carbon nanotubes show no sign of acute toxicity but induce intracellular reactive oxygen species in dependence on contaminants. *Toxicol. Lett. 168*, 58–74.

(30) Qu, G., Bai, Y., Zhang, Y., Jia, Q., Zhang, W., and Yan, B. (2009) The effect of multiwalled carbon nanotube agglomeration on their accumulation in and damage to organs in mice. *Carbon 47*, 2060–2069.

(31) Lacerda, L., Herrero, M. A., Venner, K., Bianco, A., Prato, M., and Kostarelos, K. (2008) Carbon Nanotube Shape and Individualization Critical for Renal Excretion. *Small 4*, 1130–1132.

(32) Singh, R., Pantarotto, D., Lacerda, L., Pastorin, G., Klumpp, C., Prato, M., Bianco, A., and Kostarelos, K. (2006) Tissue bio-distribution and blood clearance rates of intravenously administered carbon nanotube radiotracers. *Proc. Natl. Acad. Sci. U.S.A. 103*, 3357.

(33) Liu, Z., Davis, C., Cai, W., He, L., Chen, X., and Dai, H. (2008) Circulation and long-term fate of functionalized, biocompatible single-walled carbon nanotubes in mice probed by Raman spectroscopy. *Proc. Natl. Acad. Sci. 105*, 1410.